Thai Geoscience Journal 3(3), 2022, p. 51-58

ISSN-2730-2695; DOI-10.14456/tgj.2022.5

Cycle performance investigation in compressed air energy storage in aquifers

Lichao Yang, Cai Li, Chaobin Guo, Kai Liu, Qingcheng He*

Chinese Academy of Geological Sciences, Beijing 100037, China

***Corresponding author: 479400160@qq.com*

Received 17 March 2021; Accepted 4 July 2021.

Abstract

Compressed air energy storage (CAES) is one of the promising technologies to store the renewable energies such as surplus solar and wind energy in a grid scale. Due to the widespread of aquifers in the world, the compressed air energy storage in aquifers (CAESA) has advantages compared to the conventional CAES technologies, which store the compressed air in caverns. In this study, numerical modeling by TOUGH3/EOS3 was conducted to simulate a field-scale application of a novel CAES by storing the compressed air in an aquifer. Four types of cycles, namely daily cycle, weekly cycle, monthly cycle and seasonal cycle, were designed to study their performances. The simulation results demonstrated that the air temperature in CAESA system increases as the cycle continues. The seasonal cycle can be achieved under appropriate conditions. The air recharge should be taken to continue the seasonal cycle. The simulation results can provide references for engineering application in future.

Keywords: aquifers**,** compressed air energy storage, cycles, numerical model

1. Introduction

Renewable energies hold a lot of promise when it comes to replace the conventional energy sources such as fossil fuels. However, the intermittent feature of the power generated by renewable energies, such as wind and solar energy, will greatly constrain the utilization efficiency. Therefore, grid-scale energy storage technologies are required to improve the stability and utilization rate of the renewable energies. Among other energy storage technologies (e.g., battery and flywheel energy storage), compressed air energy storage (CAES) has been demonstrated as a promising technology for its large storage scale, economic feasibility, high reliability and low environmental influence (Oldenburg & Pan, 2013; Luo et al., 2015).

The feasibility and requirements of CAES have been proved by energy storage in air tanks, underground caverns and aquifers (Eakes et al., 1983). The Huntorf CAES project and the McIntosh CAES project are two commercial grid-scale CAES facilities with caverns operated successfully in Germany and USA, respectively (Succar & Williams, 2008; Raju et al., 2012). The compressed air energy storage in aquifers (CAESA) has advantage against compressed air energy storage in cavern due to the wide availability of aquifers as well as lower economic costs (Allen et al., 1983).

An aquifer field experiment at Pittsfield, Illinois, USA was carried out in 1981(Wiles & Mccann, 1983). The aim of this project was a feasibility demonstration of cyclical air injection and withdrawal at ambient and elevated temperatures in an aquifer reservoir (Kannberg et al., 1980; Istvan et al., 1990). The cycle of the injection and withdrawal of the air at the Pittsfield project was a daily cycle. However, the investigation on different cycle modes and their performance to CAESA system is still limited. It is therefore necessary to conduct research on different cycle modes of CAESA system to achieve the maximum utilization rate of renewable energies and meet various demands of users.

2. Model design

2.1 Conceptual model and numerical model

Compressed air was injected into an aquifer with dome-shaped anticline structure in the Pittsfield CAESA test (Wiles & McCann,

1981; Allen et al., 1983; Istvan et al., 1983). Fig. 1 shows the structure of the Pittsfield dome indicated by the contours of the uppermost Silurian formation and the well-defined closure indicated by the contours of the upper stratum. The reservoir used to store the compressed air is the highly permeable quartz-dominated St. Peter sandstone, which is beneath the impervious Gelena-Platteville-Joachim carbonate cap rock complex. The core tests showed that the cap rock formations are sufficiently impervious to hold the compressed air during the lifetime of the field test (Allen et al., 1983).

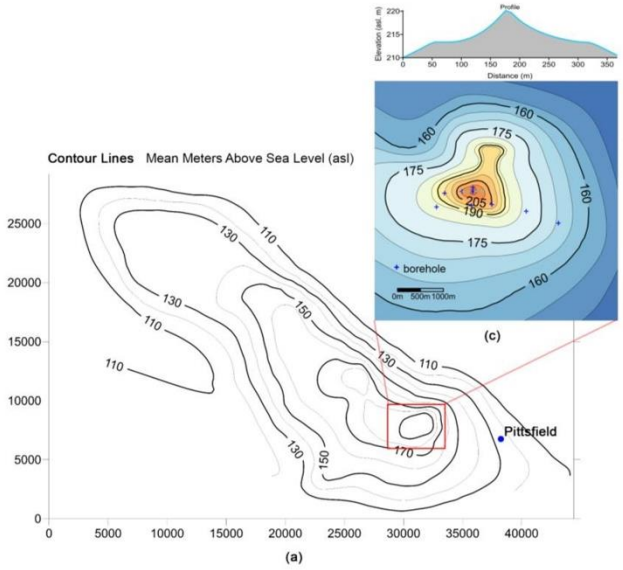

Fig. 1: The structure of the Pittsfield dome; (a) elevation contours of the uppermost Silurian formation and (b) elevation contours of the upper stratum (Allen et al., 1985).

In this study, a conceptual model was set up based on the stratigraphy of the Pittsfield site (Fig. 2). The CAESA system included two stages; the initial bubble stage and the working cycle stage. In the first stage, a large amount of compressed air was injected into an aquifer to form a large initial gas bubble (cushion gas), which was used to provide sufficient pressure and avoid water coning. In the second stage, a certain amount of compressed air was injected into the aquifer for the working cycle.

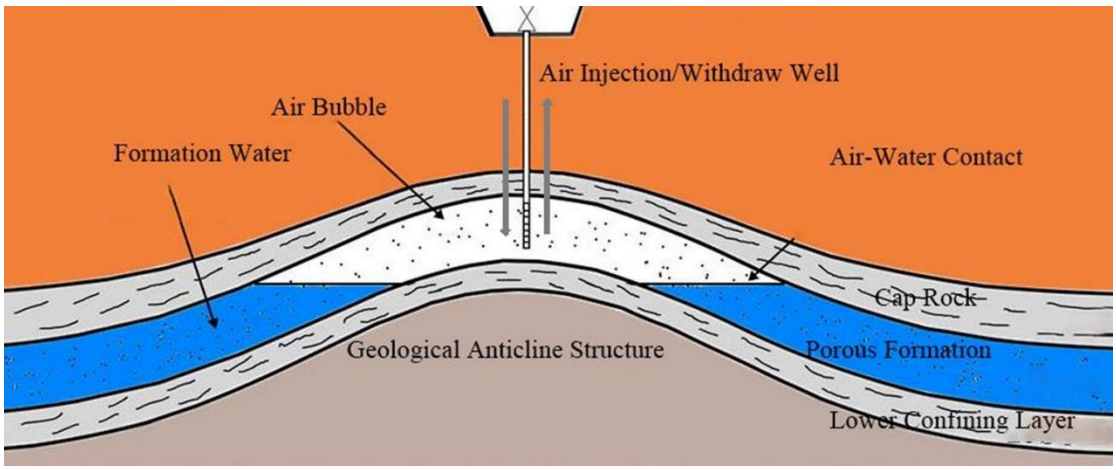

Fig. 2: Conceptual model for Pittsfield CAESA model (Wang et al., 2017).

The TOUGH3/EOS3 simulator, developed by Lawrence Berkeley National Laboratory (LBNL) in USA, was used to conduct the numerical simulations. TOUGH3 is a general-purpose numerical simulation program for multi-dimensional fluid and heat flows of multiphase, multicomponent fluid mixtures in porous and fractured media. The EOS3 module is developed to describe the system consisting of H_2O-Air-Heat components in a porous medium (Jung et al., 2021).

In the numerical modeling, the model scale is set to 3 km×3 km in the horizontal direction and 172 m in the vertical direction. Horizontally, the grids are refined gradually from the boundary to the injection/withdrawal well, which is located in the center of the model with diameter of 0.2 m (Fig. 3a and 3b). Vertically, the model includes four lithologies, which are limestone (upper layer), impervious dolomite rocks (cap rock), St. Peter sandstone (porous formation), and impervious dolomite rocks (lower confined layer), respectively (Fig. 3c). The model is divided into 35 layers vertically and the thickness for each type of lithology is 32 m, 50 m, 70 m and 20 m, respectively. In particular, the St. Peter sandstone is composed of three sub-layers, which are green layer (3 m), white layer (6 m) and grey layer (61 m), respectively (Table 1).

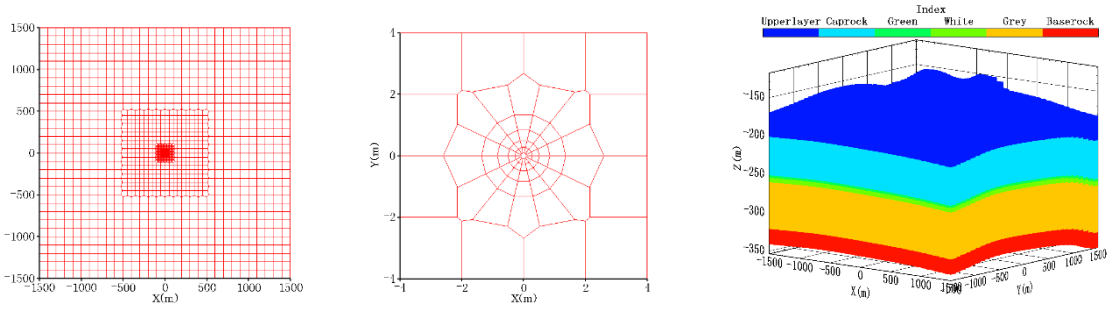

(a) (b) (c)

Fig. 3: (a) Domain discretization from boundary to wellbore in plain view, (b) wellbore refinement with wellbore diameter of 0.2 m in center, and (c) the lithologies distribution vertically in 3D view.

Table 1: Vertical layer refinement of the Pittsfield model.

Lithology	Thickness (m)		Sublayers	Thickness per layer (m)
Limestone (Upper layer)	172	32	1	2
			2	15
Dolomite rocks (Cap rock)		50	2	20
			1	6
			2	2
Sandstone (Green layer)		3	3	1
Sandstone (White layer)		6	6	1
Sandstone (Grey layer)		61	6	1
			5	2
			4	5
			1	25
Dolomite rocks (Base rock)		20	2	10

The upper and bottom boundaries were set up as constant pressure boundary. The lateral boundaries were set up as no flux boundary. In this model, the surface is set to the surface ground, where the temperature is set to 20°C and the geothermal gradient is 0.03°C/m. The initial pressure and initial temperature of this model are shown in Fig. 4. The initial pressure distribution is in hydrostatic equilibrium with atmospheric pressure at the water level, where the pressure is set as 1.01×10^5 Pa, and the hydrostatic gradient is 9.8×10^3 Pa/m.

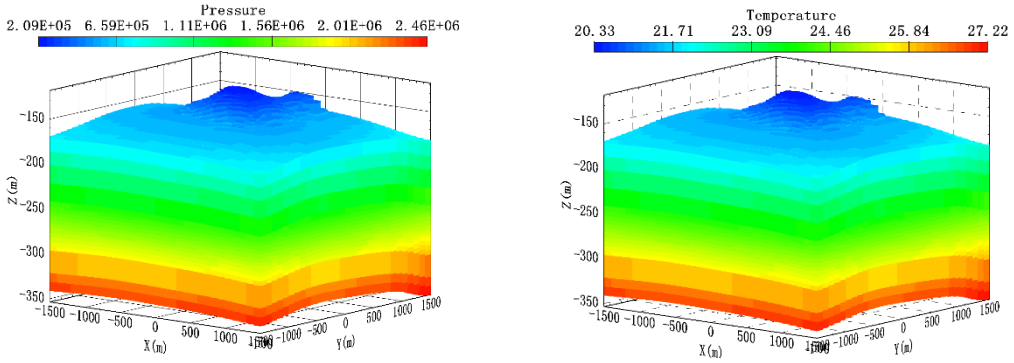

(a) (b)

Fig. 4: Initial pressure (a) and initial temperature (b) of the Pittsfield model.

2.2 Input parameters

The typical parameters for the aquifer and the injection/withdrawal (I/W) well are shown in Table 1, including permeabilities and porosities, which come from the experimental test conducted by Electric Power Research Institute (EPRI), California in the Pittsfield site (Kannberg et al., 1980; Bui et al., 1990).

Table 2: Parameters of the aquifer and wellbore.

Aquifer		**Value**		**Unit**
Grain density		2600		kg/m^3
Heat conductivity		2.16		W/m°C
Grain specific heat		920		J/kg°C
Relative permeability function		Van Genuchten-Mualem model		
Capillary pressure function		Van Genuchten function		
Residual liquid saturation (S_{lr})		0.10		
Minimal capillary pressure (P_0)		675.68		Pa
Maximal capillary pressure (P_{max})		5.0×10^5		Pa
Saturated liquid saturation (S_{ls})		1.00		
Lithology		**Porosity**	**k_h (m^2)**	**k_v (m^2)**
Sandstone	Green layer	0.17	9.05×10^{-13}	7.60×10^{-13}
	White layer	0.16	8.06×10^{-13}	6.62×10^{-13}
	Grey layer	0.16	8.70×10^{-13}	7.27×10^{-13}
Limestone	Upper layer	0.13	6.00×10^{-15}	6.00×10^{-16}
Dolomite	Cap rock & Base rock	0.13	6.00×10^{-15}	6.00×10^{-16}

3. Results and discussion

3.1 Initial bubble development

Before carrying out the working cycle, initial air bubbles need to be developed in the reservoir as cushion gas for insuring sufficient pressure and avoiding water coning (Wiles & McCann, 1981). In this model, the initial bubbles were developed with a mass flow rate of compressed air 2 kg/s and injection time of 165 days. The temperature of injection air was set to 20°C with a fixed specified enthalpy. Fig. 5 shows the gas saturation of the initial bubbles after 165 days injection. The injection point is located at the bottom of the I/W well, where the red dot corresponds to in Fig. 5. It states that the plume of bubbles, where the gas saturation is 0.3, can reach up to 650 m in the horizontal direction, and the biggest thickness of the bubble is about 70 m in the vertical direction.

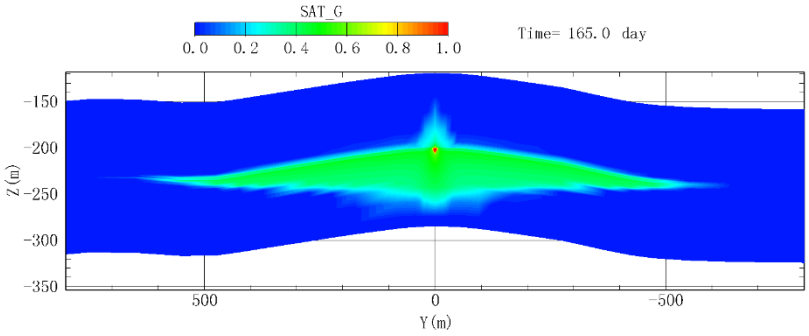

Fig. 5: Gas saturation at the initial bubble development after 165 days air injection.

3.2 Mass flow rates of designed cycles

The daily cycle was designed to 12 hours injection and 12 hours production (Fig. 6a), the weekly cycle was 3.5 days injection and 3.5 days production (Fig. 6b), the monthly cycle was 14 days injection and 14 days production (Fig. 6c), and the seasonal cycle was 90 days injection, 90 days shut-in, 90 days production and 90 days shut-in (Fig. 6d). The mass flow rates of the daily cycle, weekly cycle and monthly cycle were all 2 kg/s, and 1 kg/s for seasonal cycle.

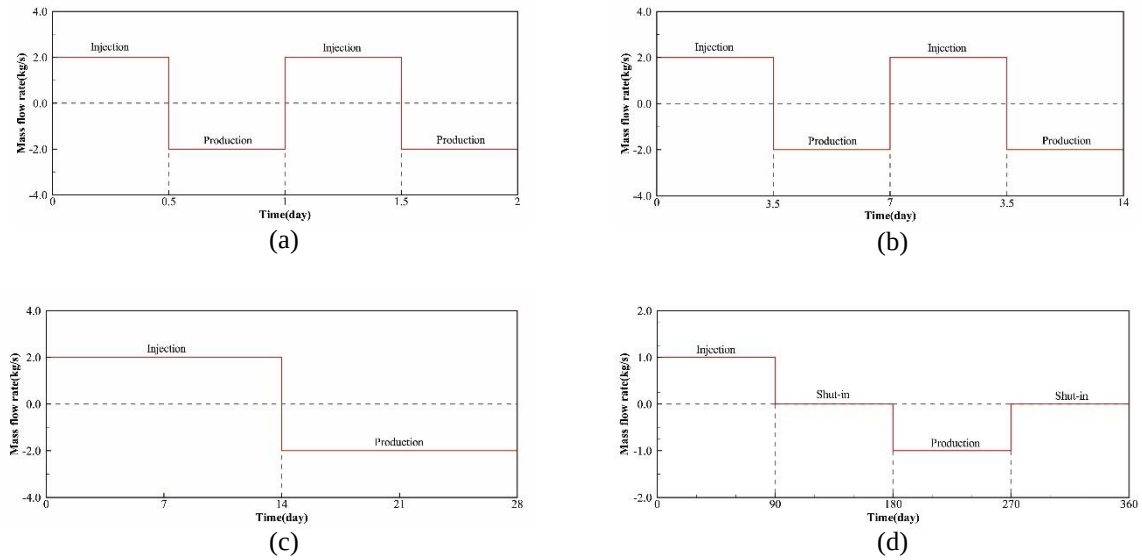

Fig. 6: The mass flow rate of four designed cycles. Minus values stand for production process.

3.3 Pressure and temperature performance of three designed cycles

Before the working cycle, the pressure in the aquifer at point r_1 (0.2 m away from the bottom of the I/W well) was 4.17 MPa, and the temperature is 22.78°C. After one month's simulation, the pressure at r_1 became 1.49 MPa, 1.44 MPa and 1.43 MPa for daily cycle, weekly cycle and monthly cycle, respectively (Fig. 7). It indicates that the energy loss in daily cycle is the smallest because the daily cycle has the shortest period.

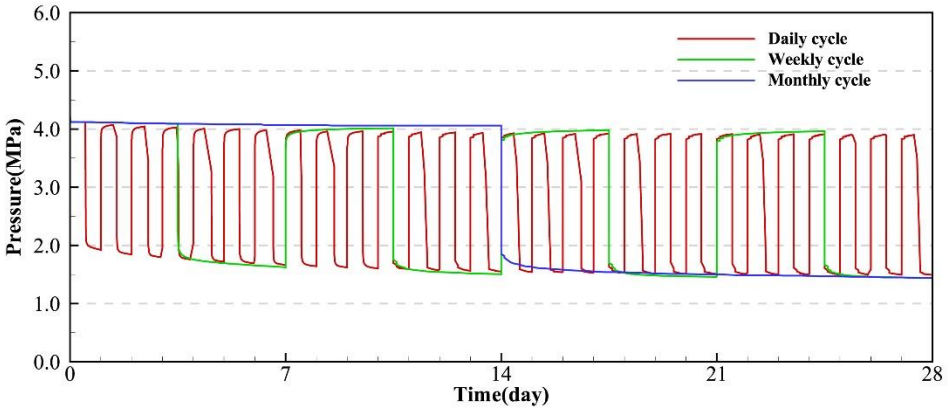

Fig. 7: Pressure variations in daily cycle, weekly cycle and monthly cycle in the aquifer at point r_1 (0.2 m away from the bottom of the I/W well).

The temperature of the air injected into the I/W well was 50°C with a fixed enthalpy. Fig. 8 shows the temperature variation of three types of cycles. When the cycles of 28 days were finished, the air temperature at r_1 was 39°C, 33.6°C and 28.2°C for daily cycle, weekly cycle and monthly cycle, respectively. It indicates that during the same working cycle, the temperature in the aquifer increases as the cycle continues.

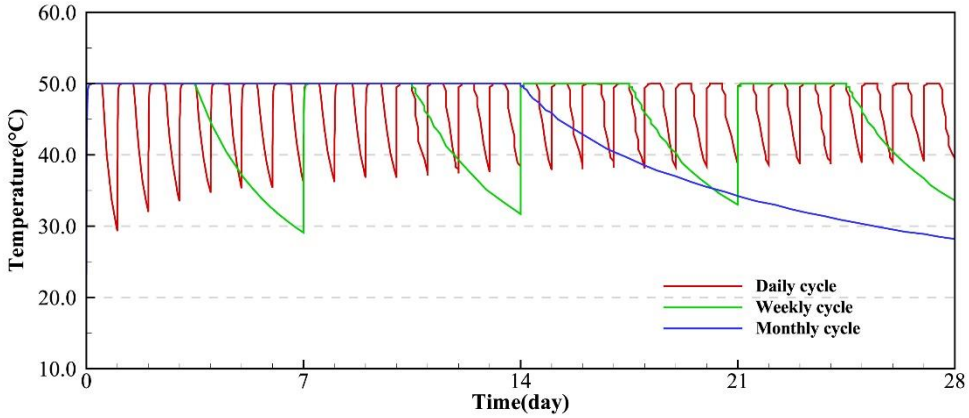

Fig. 8: Temperature variations in daily cycle, weekly cycle and monthly cycle at point r_1 in the aquifer.

3.4 Pressure and temperature performance of seasonal cycle

Fig. 9 shows the pressure variation at points r_1, r_2 and r_3, which were in the aquifer and 0.2 m, 1 m and 100 m, respectively, away from the bottom of the I/W well.

Before the air injection, the pressure at r_1 is 4.17 MPa (overlapped with Y-axis). During the injection stage (A to B), the energy spreads to surroundings gradually, so the pressure decreases in the early stage. As the air injection continued, the rates of energy loss decreased, then the pressures increased to 3.7 MPa, 3.48 Mpa, and 3.19 Mpa at r_1, r_2 and r_3, respectively. During the shut-in stage (B to C), the pressure decreased suddenly because the injection rate decreased to zero, and then the pressure basically became stable in the shut-in stage. During the production stage (C to D), firstly the

pressure decreased because of the sudden air withdrawal, and then kept decreasing as the production continued. When the air production finished, the pressure at r_1, r_2 and r_3 were 1.93 MPa, 2.51 MPa and 2.85 MPa, respectively. During the second shut-in stage (D to E), the pressure recovered firstly, and then basically kept stable. It can be seen that the pressure loss in the I/W well at the end of one cycle was too large to continue the cycle, so in this study, the recharge of compressed air was needed to continue the cycles.

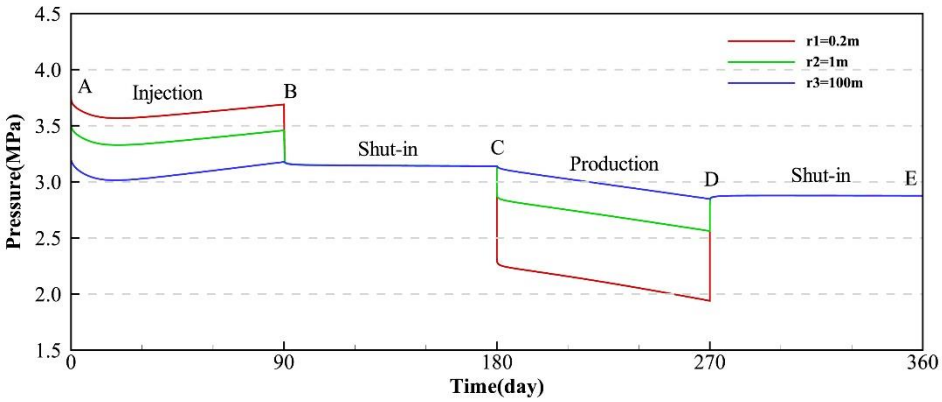

Fig. 9: Pressure variation of seasonal cycle at different sites.

Fig. 10 shows the temperature variation at r_1, r_2 and r_3. The injection air temperature was 50°C. During the injection stage (A to B), the temperature at r_1 was 50°C due to the small distance from the bottom of I/W well. The temperature at r_2 increased from 30°C to 49°C, while the temperature at r_3 kept 22.8°C during the whole cycle because of the long distance from the I/W well. During the shut-in stage (B to C), the temperature at r_1 and r_2 decreased to 38 °C and 35.9°C because of the temperature transfer from high to low. During the production stage (C to D), the temperature decreased gradually, and the temperature at r_1 and r_2 decreased to 25.1°C and 24.9°C when the air production finished. During the second shut-in stage, the high temperature air had been withdrawn, so the temperature in the aquifer had no big difference, with 25.5°C both at r_1 and r_2.

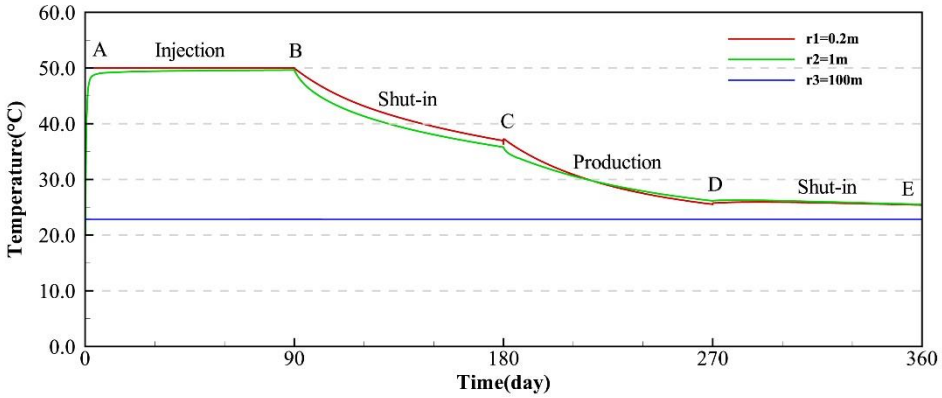

Fig. 10: Temperature variation of seasonal cycle at different sites.

4. Conclusions

In this study, a numerical model was built to investigate the performance of various injection and withdrawal cycles of CAESA: daily, weekly, monthly and seasonal cycles. The modelling results show that during the same working cycle, the temperature of the aquifer increases as the cycle repeats. In addition, the seasonal cycle can be achieved with appropriate conditions, but recharge of the compressed air is needed to continue the cycle due to the large pressure loss. In a practical CAESA project in future, the working cycle

should be designed according to specific characteristics of renewable energy and the actual power demands of users. A comprehensive consideration should be placed to choose the most cost-efficient CAESA system. There are still many fundamental issues for the CAESA system research. With regard to the study and field operation in future, more attention should be paid to the characterization of the reservoir structure. The CAESA system performance largely depends on the aquifers' properties, especially the permeability and porosity.

Acknowledgments

The authors gratefully acknowledge the funding support from the Chinese Academy of Geological Sciences, China (Grant No. DD20201165 and No. JKY202004). The authors also gratefully thank to all the reviewers of their thorough comments.

References

Allen, R. D., Doherty, T. J., Erikson, R. L., & Wiles, L. E. (1983). Factors affecting storage of compressed air in porous-rock reservoirs. technical report.

Allen, R. D., Doherty, T. J., & Kannberg, L. D. (1985). Summary of selected compressed air energy storage studies. technical report.

Eakes, R. G., Kempka, S. N., & Lamoreaux G. H. (1983). Review of environmental studies and issues on compressed air energy storage. technical report.

Wang, B., & Bauer, S. (2017). Pressure response of large-scale compressed air energy storage in porous formations. *Energy Procedia*, 125, 588-595.

Bui, H. V., Herzog, R. A., Jacewicz, D. M., Lange, G. R., Scarpace, E. R., & Thomas, H. H. (1990). Compressed-air energy storage: Pittsfield aquifer field test. technical report.

Istvan, J. A., Crow, C. V., Pereira, J. C., & Bakhtiari, H. (1983). Compressed Air Energy Storage (CAES) in an Aquifer - A Case History. Soc.pet.eng.aime Pap; (United States).

Istvan, J. A., Pereira, J. C., Roark, P., & Bakhtiari, H. (1990). Compressed-air energy storage field test using the aquifer at Pittsfield, Illinois. technical report.

Jung, Y., Pau, G., Finsterle, S., & Doughty, C. (2021). TOUGH3 User's Guide, Version 1.0. Lawrence Berkeley National Laboratory.

Kannberg, L. D., Doherty, T. J., & Allen, R. D. (1980). Aquifer field test for compressed air energy storage. Proc., Intersoc. Energy Convers. Eng. Conf.; (United States).

Luo, X., Wang, J., Dooner, M., & Clarke, J. (2015). Overview of current development in electrical energy storage technologies and the application potential in power system operation. *Applied Energy*, 137, 511-536.

Oldenburg, C. M., & Pan, L. (2013). Porous Media Compressed-Air Energy Storage (PM-CAES): Theory and Simulation of the Coupled Wellbore–Reservoir System. *Transport in Porous Media*, 97(2), 201-221.

Raju, M., & Khaitan, S. K. (2012). Modeling and simulation of compressed air storage in caverns: A case study of the Huntorf plant. *Applied Energy*, 2012,89(1), 474-481.

Succar, S., & Williams, R. H. (2008). Compressed air energy storage: theory, resources, and applications for wind power, Princeton Environmental Institute.

Wiles, L. E., & McCann, R. A. (1981). Water coning in porous media reservoirs for compressed air energy storage. technical report.

Wiles, L. E., & Mccann, R. A. (1983). Reservoir characterization and final pre-test analysis in support of the compressed-air-energy-storage Pittsfield aquifer field test in Pike County, Illinois. technical report.